MINDO/3 Calculations on the Acid-Catalyzed Ring Opening of Oxaziridine

James F. Garvey and Joseph A. Hashmall*

Department of Chemistry, Georgetown University, Washington, D.C. 20057

Received June 27, 1977

MINDO/3 semiempirical molecular orbital calculations were performed on oxaziridine and four protonated derivatives (N-protonated, O-protonated cis, O-protonated trans, and edge protonated). For the first three of these, further calculations were done along reaction coordinates, leading to ring cleavage at each of the three possible bonds. The results are interpreted to favor a mechanism for the ring opening of *N*-alkyloxaziridines which goes through the O-protonated intermediate, while in a *C*-phenyl derivative a mechanism with an N-protonated intermediate is favored. Reaction coordinates for the intramolecular interconversion of the four protonated derivatives were also calculated.

Oxaziridines (derivatives of 1) decompose rapidly in acid medium to form acyclic products. This reaction is interesing because oxaziridine is a small molecule with several possible protonation sites (N, O, and the ring edge). The two mechanisms proposed for this reaction[1,2] have as their initial step protonation at the oxygen. Substitution of a carbonium ion stabilizing group, such as phenyl, at the ring carbon changes the products from those of eq 1 to those of eq 2.

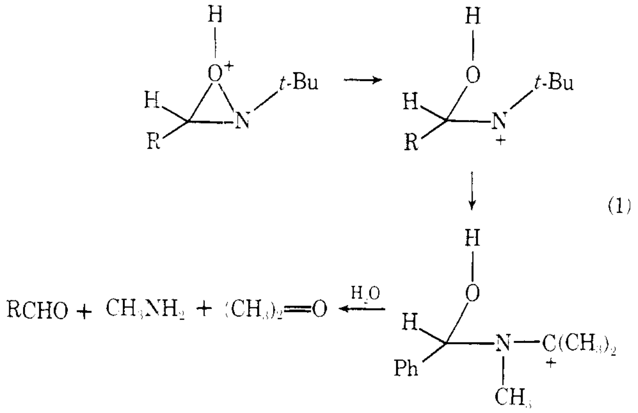

(1)

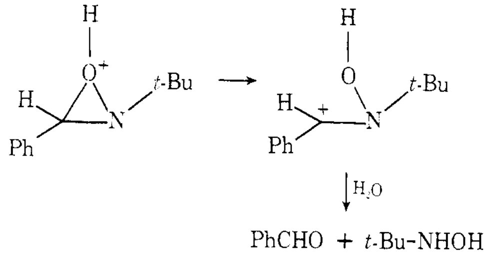

(2)

Ab initio molecular orbital calculations on this system indicate nitrogen as the favored site for protonation,[3] and a recent study of the $AgBF_4$ complex of an oxaziridine derivative indicates nitrogen as the preferred site for Ag^+ complexation.[4] A third mechanism (eq 3), with initial N-protonation, can also explain the products which would be given by eq 2.

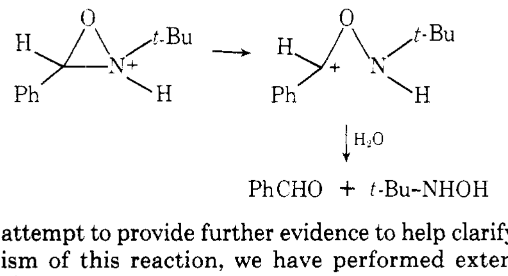

(3)

In an attempt to provide further evidence to help clarify the mechanism of this reaction, we have performed extensive MINDO/3 calculations[5] on the potential energy surface of protonated oxaziridine.

Calculations. MINDO/3 calculations were performed on oxaziridine (1), N-protonated oxaziridine **2**, cis and trans O-protonated oxaziridines (**3** and **4**), and oxaziridine protonated on the N–O bond (**5**).

CN and CO edge-protonated species were not calculated because they were expected to be significantly less stable than **5**, which itself has only a very shallow potential well. The calculated energies and charge densities of each of these species are presented in Table I, and their structures, found by minimization of the MINDO/3 energy of each species with respect to all geometry parameters (bond lengths, angles, and twist angles), are presented in Figure 1.

For species **2–4** calculations were then carried out on the species with each of the three ring bonds separately stretched. For each constant distance of the single ring bond which was stretched, all other geometry parameters were optimized to give a point on the reaction coordinate leading to ring opening by cleavage of one bond. This procedure was repeated with successive small increments until a transition state was found. Once each transition state was passed, all geometry parameters were again optimized to obtain product geometries. In all, nine reaction coordinates of this type were followed, involving several thousand MINDO/3 calculations.

In addition to the nine reaction coordinates described above, reaction coordinates for cis–trans isomerization of the O-protonated species, and for the intramolecular O–N proton transfer reaction, starting with either cis or trans O-protonated oxaziridine were calculated.

Results

The nine reaction paths were labeled as

NHCN: N-protonated, C–N bond cleavage
NHON: N-protonated, O–N bond cleavage
NHCO: N-protonated, C–O bond cleavage
COHCN: cis O-protonated, C–N bond cleavage
COHON: cis-O-protonated, O–N bond cleavage
COHCO: cis O-protonated, C–O bond cleavage
TOHCN: trans O-protonated, C–N bond cleavage
TOHON: trans O-protonated, O–N bond cleavage
TOHCO: trans O-protonated, C–O bond cleavage

The geometries of the transition states and the products of eight of these ring cleavage steps are summarized in Figures 2–4. Path NHCO was followed to a C–O bond length of 2.8 Å (289.6 kcal/mol). At longer C–O distances the SCF procedure did not converge.

The transition states for cis–trans isomerization of the O-protonated species and for the O to N proton transfer reactions are given in Figure 5. Energies and charge densities for each species in the figures are presented in Table I. Complete geometry data for each of the 21 intermediates and transition states are presented in the supplementary material.

0022-3263/78/1943-2380$01.00/0

Table I. Calculated Energies and Charge Densities

Compd	ΔE_f, kcal/mol	q_C	q_N	q_O	q_{H_1}	q_{H_2}	q_{H_3}	q_{H_4}
1	0.4	+0.38	+0.07	−0.35	−0.06	−0.06	+0.02	
2	173.7	+0.36	+0.35	−0.20	+0.08	+0.08	+0.16	+0.16
3	181.6	+0.34	+0.22	−0.16	+0.10	+0.06	+0.12	+0.33
4	182.7	+0.36	+0.18	−0.17	+0.08	+0.04	+0.14	+0.34
5	200.9	+0.38	+0.15	−0.20	+0.09	+0.08	+0.15	+0.35
6	208.4	+0.77	+0.18	−0.30	+0.03	+0.03	+0.15	+0.15
7	253.6	+0.38	+0.29	−0.09	+0.05	+0.05	+0.16	+0.16
8	186.1	+0.66	+0.32	−0.28	+0.05	+0.05	+0.10	+0.10
9	133.0	+0.91	−0.14	−0.14	+0.23	+0.23	0.00	+0.00
10	263.3	+0.51	−0.01	−0.08	+0.11	+0.07	+0.08	+0.33
11	212.3	+0.35	+0.34	−0.27	+0.02	+0.10	+0.14	+0.32
12	211.2	+0.42	+0.22	−0.23	+0.06	+0.11	+0.12	+0.30
13	261.1	+0.46	−0.05	−0.02	+0.13	+0.08	+0.07	+0.33
14	106.1	+0.62	−0.04	−0.35	+0.05	+0.18	+0.19	+0.34
15	167.8	+0.09	+0.50	−0.32	+0.16	+0.14	+0.10	+0.33
16	264.4	+0.51	−0.03	−0.10	+0.11	+0.07	+0.10	+0.35
17	205.6	+0.37	+0.29	−0.28	+0.08	+0.07	+0.15	+0.21
18	216.0	+0.48	+0.14	−0.23	+0.07	+0.08	+0.15	+0.32
19	194.9	+0.42	+0.24	−0.31	+0.06	+0.07	+0.11	+0.40
20	202.6	+0.36	+0.17	−0.16	+0.06	+0.12	+0.11	+0.34
21	204.5	+0.47	+0.17	−0.19	+0.08	+0.09	+0.15	+0.33

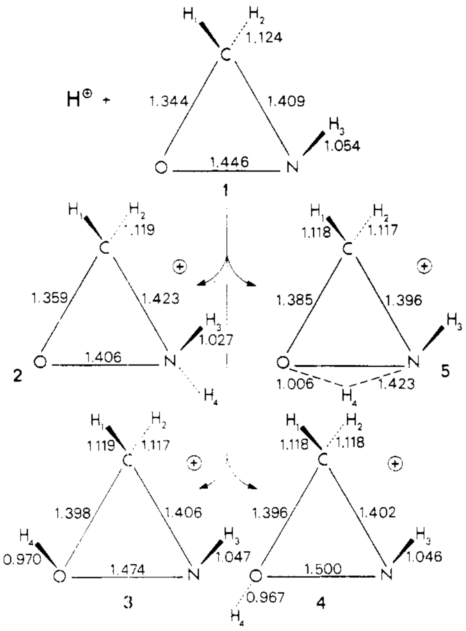

Figure 1. Calculated structures of oxaziridine (1) and four protonated oxaziridines (2–5).

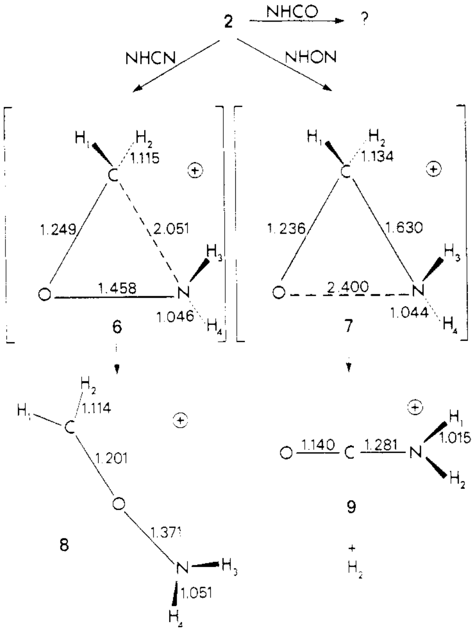

Figure 2. Calculated structures of the transition states and products for the ring openings of N-protonated oxaziridine (2).

Several important points should be noted. (1) Nitrogen is predicted to be the preferred site of protonation, as shown in Table I with the energies of N-protonated species **2** at 173.7 kcal/mol, cis O-protonated **3** at 181.6 kcal/mol, trans O-protonated **4** at 182.7 kcal/mol, and N–O edge-protonated **5** at 200.9 kcal/mol.

(2) The preferred reaction path is through the O-protonated species, but the energy differences between O-protonated and N-protonated transition states are probably too small to be significant. These path preferences are obtained by comparison of the energies of transition states: **6**, 208.4 kcal/mol; **11**, 212.3 kcal/mol; **12**, 211.2 kcal/mol; **17**, 205.6 kcal/mol; and **18**, 216.0 kcal/mol.

(3) Transition states for intramolecular proton transfer reactions (including the cis–trans isomerization) are of lower energy than those of the ring cleavage reactions: **19**, 194.9 kcal/mol; **20**, 202.6 kcal/mol; and **21**, 204.5 kcal/mol. Intermolecular proton transfer probably requires less activaion energy.

(4) The COHON and TOHON paths produced products in which a proton has moved from the ring carbon to the nitrogen.

(5) Path NHON (which has a high energy transition state) results in products formed by loss of a molecule of hydrogen from the organic compound. Loss of H_2 as well as the proton transfer described in point 4 were results of the calculations. They were not assumed paths.

(6) The products of path COHCN differ from those of TOHCN by rotations around single bonds; the energies are essentially identical. The same relation holds between the products of paths COHCO and TOHCO, and the products of paths COHON and TOHON are identical.

(7) The O to N proton transfer reaction goes through a transition state to a shallow minimum when starting from the

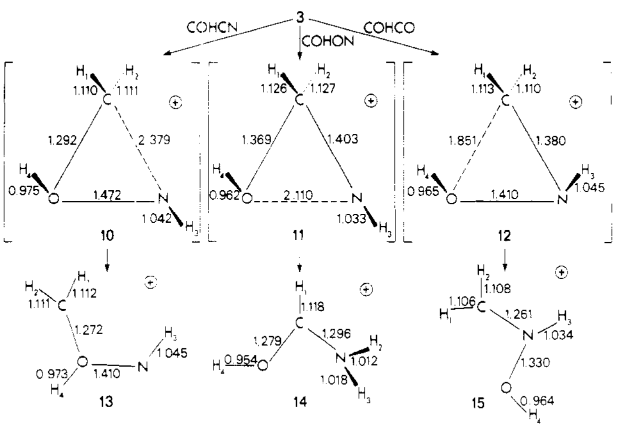

Figure 3. Calculated structures of the transition states and products for the ring openings of cis O-protonated oxaziridine (**3**).

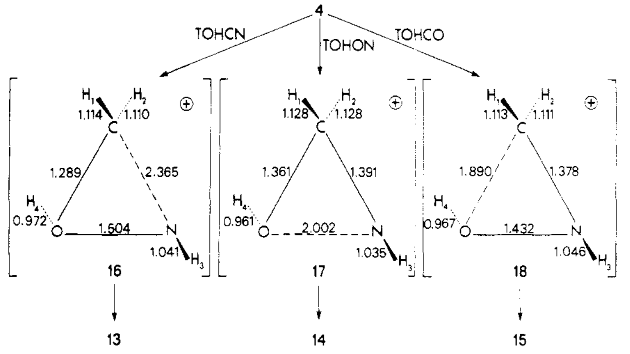

Figure 4. Calculated structures of the transitions states and products for the ring openings of trans O-protonated oxaziridine (**4**).

trans O-protonated species. This minimum is the edge-protonated species **5**. Further progress along this reaction path leads to a second transition state which is identical with that for the cis O-protonated to N proton transfer reaction which has no minimum along the reaction coordinate.

Discussion

Care must be used in using molecular orbital calculations to interpret reactions in solution. To make this type of interpretation, one must assume that solvent effects cancel. In the present case it would be futile, from the calculations, to try to predict the energy changes of the protonation reaction, but the energies of the four protonated intermediates (**2–5**) may reasonably be compared using the assumption that each is similarly solvated. This assumption is perhaps more valid in the case of charged species, such as studied here, because the major solvation interaction is a charge–dipole interaction, which would be similar for species with similar net charges and similar geometries in the vicinity of the charge.

Errors due to the inability of the MINDO/3 method to account for strain energy preclude the comparison of cyclic with acyclic species, but the three-membered ring intermediates may be compared with each other. Comparison may also be made between ring opening transition states if the transition state is about equally far from the starting material in each case.

The results show that the N-protonated species is somewhat more stable than any other protonated species, in agreement with the experimental and computational conclusions referred to above. Paths NHON, NHCO, COHCN, and TOHCN are clearly of too high an energy to be important in the actual reactions. The remaining five paths are of similar enough energy to allow minor changes in structure and substitution to alter the preferred path among them. Proton transfer among the protonated oxaziridines appears to be somewhat faster than the ring opening reactions.

In two of the paths (COHON and TOHON) proton transfer from the ring carbon to the nitrogen occurs in the course of the reaction. For the reaction with a *tert*-butyl group on the nitrogen, CH_3^+ is transferred (as in reaction 1). Both types of transfer are possible in the *N-tert*-butyl system, so the observation of products resulting exclusively from methyl transfer indicates that the transition state including this process is at a lower energy than that with proton transfer. Therefore, for *N*-alkyloxaziridines eq 1 is predicted to be the favored mechanism.

The transition state for path NHCN (**6**) shows a considerable increase of positive charge compared to its precursor **2**. This charge localization, the difference between q_C for **6** (+0.77) and q_C for **2** (+0.36), is +0.41. An aryl substituent on the carbon will stabilize the positive charge of **6** more than the smaller positive charge on **2**. The activation energy for path NHCN will therefore be lowered by aryl substitution. A similar but smaller effect is seen in paths COHCO (q_C: **12**, 0.42; **3**, 0.34; $\Delta q_C = 0.08$) and TOHCO (q_C: **18**, 0.48; **4**, 0.36; $\Delta q_C = 0.12$), which indicates less decrease in the activation energy for these paths.

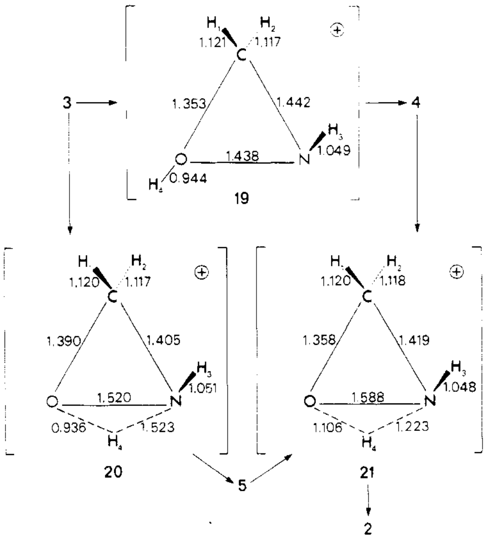

Figure 5. Calculated structures of the transition states for intramolecular proton transfer of protonated oxaziridines.

The resonance stabilization of a positive charge by a phenyl group can be obtained by comparing the experimental enthalpies of the reactions shown in eq 4–10. Assuming that the transition state stabilization is proportional to the increment of positive charge at the carbon atom, a phenyl group would lower the activation energy of path COHCO by 5.6 kcal/mol, of path TOHCO by 8.4 kcal/mol, and of path NHCN by 28.7 kcal/mol. For the phenyl derivative this last path seems most probable.

$$CH_4 \rightarrow CH_3\cdot + H\cdot \quad 103\ \text{kcal/mol}^{6} \tag{4}$$

$$CH_3\cdot \rightarrow CH_3^+ + e^- \quad 226\ \text{kcal/mol}^{7} \tag{5}$$

$$CH_4 \rightarrow CH_3^+ H\cdot + e^- \quad 329\ \text{kcal/mol} \tag{6}$$

$$PhCH_3 \rightarrow PhCH_2\cdot + H\cdot \quad 83\ \text{kcal/mol}^{8} \tag{7}$$

$$PhCH_2\cdot \rightarrow PhCH_2^+ + e^- \quad 176\ \text{kcal/mol}^{9} \tag{8}$$

$$PhCH_3 \rightarrow PhCH_2^+ + H\cdot + e^- \quad 259\ \text{kcal/mol} \tag{9}$$

$$\text{Net: } CH_3^+ + PhCH_3 \rightarrow CH_4 + PhCH_2^+ \ -70\ \text{kcal/mol} \tag{10}$$

Conclusions

Within the uncertainties stated above, it appears probable that N-protonation of oxaziridine is somewhat favored over

O-protonation and considerably favored over edge protonation. The various protonated species are in equilibrium with each other, and this intramolecular equilibrium is probably somewhat faster than the ring opening. Intermolecular equilibrium among the protonated species may well be faster still. The three postulated mechanisms are similar in transition state energies for oxaziridine itself, but N-alkylation can be expected to favor eq 1 (O-protonation followed by O–N bond cleavage) over the others. Since it is observed that substitution of an aryl group at the carbon changes the products from those expected for eq 1 to those which would be expected for eq 2 or 3 and since aryl substitution is predicted to favor eq 3 far more than it does eq 2, it seems probable that the observed products result from eq 3 rather than 2. The previously accepted mechanism involving O-protonation followed by C–O bond cleavage is less supported by the calculations than is the mechanism involving N-protonation followed by C–N bond cleavage.

Acknowledgment. We wish to thank Dr. DeLanson R. Crist for many helpful discussions and the Georgetown University Central Computer Facility for providing access to its IBM 370/145 computer on which this work was done.

Registry No.—**1**, 32201-41-5.

Supplementary Material Available: A complete listing of the optimized geometry parameters of species **1**–**21** (8 pages). Ordering information is given on any current masthead page.

References and Notes

(1) W. D. Emmons, *J. Am. Chem. Soc.*, **79**, 5739, (1957).

(2) A. B. Butler and B. C. Challis, *J. Chem. Soc. B*, 778, (1971).

(3) C. Ghio and J. Tomasi, *Theor. Chim. Acta*, **30**, 151, (1973).

(4) D. R. Crist, G. J. Jordon, and J. A. Hashmall, *J. Am. Chem. Soc.*, **96**, 4927, (1974).

(5) R. C. Bingham, M. J. S. Dewar, and D. H. Lo, *J. Am. Chem. Soc.*, **97**, 1285, (1975).

(6) F. P. Lossing, K. U. Ingold, and J. H. S. Henderson, *J. Chem. Phys.*, **22**, 1489, (1954).

(7) W. A. Chupka and C. Lifshitz, *J. Chem. Phys.*, **48**, 1109 (1968).

(8) A. H. Sehon and M. Szwarc, *Annu. Rev. Phys. Chem.*, **8**, 439, (1957).

(9) F. A. Elder and A. C. Parr, *J. Chem. Phys.*, **50**, 1027 (1969).

Steric Effects. 12. Substituents at Phosphorus

Marvin Charton* and Barbara I. Charton

Department of Chemistry, Pratt Institute, Brooklyn, New York 11205

Received August 19, 1977

Ionization constants of four sets of alkyl-substituted phosphorus oxy acids, rate constants for hydrolysis of four sets of alkyl-substituted phosphorus oxy acid esters, rate constants for the reaction of 22 sets of XZ(PO)Cl with water, and rate constants for the reaction of a set of trialkylphosphines with ethyl iodide have been correlated with both the υ and the υ' steric parameters by means of the modified Taft equation. The pK_as gave best results with the υ parameters, in accord with the tetrahedral geometry of the acids. The rate constants for the reaction of XZ(PO)Cl with water are best correlated by the υ' constants, the results in agreement with a transition state exhibiting trigonal-bipyramidal geometry with the nucleophile and leaving group at opposite positions. The success of the correlations with the υ or υ' steric parameters shows that significant steric effects occur in the acidity of phosphonic and phosphinic acids, the reaction of derivatives of these acids with nucleophiles, and the reaction of trialkylphosphines with ethyl iodide. Furthermore, steric parameters evaluated from reactions of carbon compounds may be successfully applied to the reactivity of compounds of phosphorus. The $\sigma\phi$ constants proposed by Kabachnik for use with substituents at phosphorus were correlated with $\sigma\phi_X = L\sigma_{IX} + D\sigma_{RX} + S\upsilon_X + c$ with excellent results. The steric term was significant at the 99.9% confidence level. The results show clearly that substituents exert the same types of electrical effects at phosphorus that they do when bonded to carbon. They also provide verification for the conclusion that υ values for alkoxy, alkylthio, and dialkylamino groups are on the same scale as the υ values for other substituents.

We have hitherto studied the steric effect of alkyl substituents attached to oxygen[1] and to nitrogen[2] in carbonyl compounds and alkyl groups attached to sulfur[3] in a variety of compounds. In this work we turn our attention to steric effects of alkyl groups attached to phosphorus. We have examined the correlation with the modified Taft equation[1–3]

$$Q_X = S\upsilon_X + h \qquad (1)$$

with the pK_as for four sets of alkyl-substituted phosphorus oxy acids; four sets of rate constants for the hydrolysis of esters of alkyl-substituted phosphorus oxy acids; 22 sets of rate constants for reactions of alkyl-substituted acyl chlorides of phosphorus oxy and thio acids with water; and one set of rate constants for the reaction of trialkyl phosphines with ethyl iodide. The data used in the correlations are reported in Table I. We have considered only steric effects on the reactions studied because the magnitude of the localized (field and/or inductive) electrical effect as measured by reliable σ_I values[4] for nine alkyl groups (Me, Et, Pr, *i*-Pr, Bu, *i*-Bu, *s*-Bu, and *t*-Bu) is −0.01 ± 0.02. The magnitude of the delocalized (resonance) electrical effect as determined by reliable σ_R values[4] for four alkyl groups is −0.16 ± 0.02. These values lead to the inexorable conclusion that the electrical effects of alkyl groups are constant and independent of alkyl group structure. This view is supported by our previous work.[5,6]

There are two different sets of υ parameters for alkyl groups available: the υ values derived from rate constants for esterification of carboxylic acids[7,8] and the υ' values derived from the reaction of alkyl carbinyl bromides with bromide ion.[9] These constants differ in their sensitivity to branching in the alkyl group.[10] The υ parameters reflect steric effects in a tetrahedral species while the υ' parameters represent steric effects in the S_N2 transition state which may be considered as a trigonal bipyramid. We have examined the correlation of all the data with both types of steric parameter and some results of the correlations for those sets with five or more points. [For complete statistics for all the sets studied, see the paragraph at the end of this paper about the supplementary material.] Sets designated A were correlated with υ and sets designated B were correlated with υ' values. We found it necessary to estimate a value of υ' for the *s*-Bu group for use with several of the sets studied. To accomplish this, we have assumed addi-

0022-3263/78/1943-2383$01.00/0